Journal of Science and Transport Technology

University of Transport Technology

Nonlinear buckling analysis of FGM plates stiffened by different FGM stiffener types

Dang Viet Tuan[1], Dao Quang Huy[2]

[1]Construction Engineering Faculty, University of Transport and Communications, Hanoi 100000, Vietnam

[2]Faculty of Civil engineering, University of Transport Technology, Hanoi 100000, Vietnam

Article info

Type of article:

Original research paper

Corresponding author:

E-mail address:

huydq@utt.edu.vn

Received: 31/8/2022

Accepted: 20/9/2022

Published: 25/9/2022

Abstract: In this paper, the nonlinear buckling behavior of functionally graded material (FGM) plates subjected to an axial compression is analytically investigated. Assuming that the plates are stiffened by FGM rectangular, I- and T-stiffeners. The formulations are established by using the classical plate theory considering the geometrical nonlinearities of von Karman. The Lekhnitskii's smeared stiffener technique is developed for different types of FGM stiffeners. The Galerkin method is utilized to obtain the algebraically nonlinear equation system, then, solve it to determine the explicit expressions of critical buckling loads and postbuckling load–deflection curves of plates. Numerical examples validate the effects of different types of FGM stiffeners, material and geometrical parameters on nonlinear behavior of plates.

Keywords: Functionally graded material; Stiffener; Nonlinear buckling; Axial compression; Plate; Classical plate theory.

1. Introduction

The structures in the form of plate are the basic engineering structures in many areas as mechanical engineering, civil engineering, and other engineering structures. Today, because of the engineering requirements, the studies and real applications of advanced composite materials are very popular. Functionally graded material (FGM) [1] is an advanced composite material which has the thermo-mechanical properties varying continuously from one surface to the other. The superior properties of FGM give a great advantage in the possibility of being selected in practice.

The bending, mechanical and thermal buckling and postbuckling analysis of unstiffened FGM plates were investigated using different theories and method by many authors [2-5]. The static and dynamic buckling behavior of FGM plates stiffened by isotropic and FGM rectangular stiffeners was studied [6, 7]. For isotropic rectangular stiffeners, the Lekhnitskii's smeared stiffener technique was applied [6] and the improved technique was developed for FGM rectangular stiffeners [7]. For oblique FGM stiffeners, others improved smeared stiffener techniques were presented according to the first- and higher-shear deformation theory [8,9].

Due to the engineering requirements, the different geometrical forms of stiffeners needs to be considered. This paper proposes a new designs for FGM I- and T-Stiffeners, and an analytical approach for nonlinear buckling and postbuckling of FGM plates stiffeners by FGM rectangular, I- and T-Stiffeners under axial compression is presented. The improved Lekhnitskii's smeared stiffener technique is applied for three stiffener types of

FGM stiffeners within the framework of classical plate theory. A very large effects of geometrical and material parameters of stiffeners are obtained on the buckling and postbuckling behavior of the plates.

2. FGM plates stiffened by different FGM stiffener types and solution procedure

Consider a stiffened FGM plate of length a, width b and thickness h which is subjected to axial compressive load r_0. The plate is reinforced by stiffener system included longitudinal and transversal FGM stiffeners with the geometrical parameters presented in Fig. 1. The mid-plane of plate skin is referred to the coordinate (x,y,z), and the cross-sections of T- and I-Stiffeners are respectively divided into two and three parts as shown in Fig. 1.

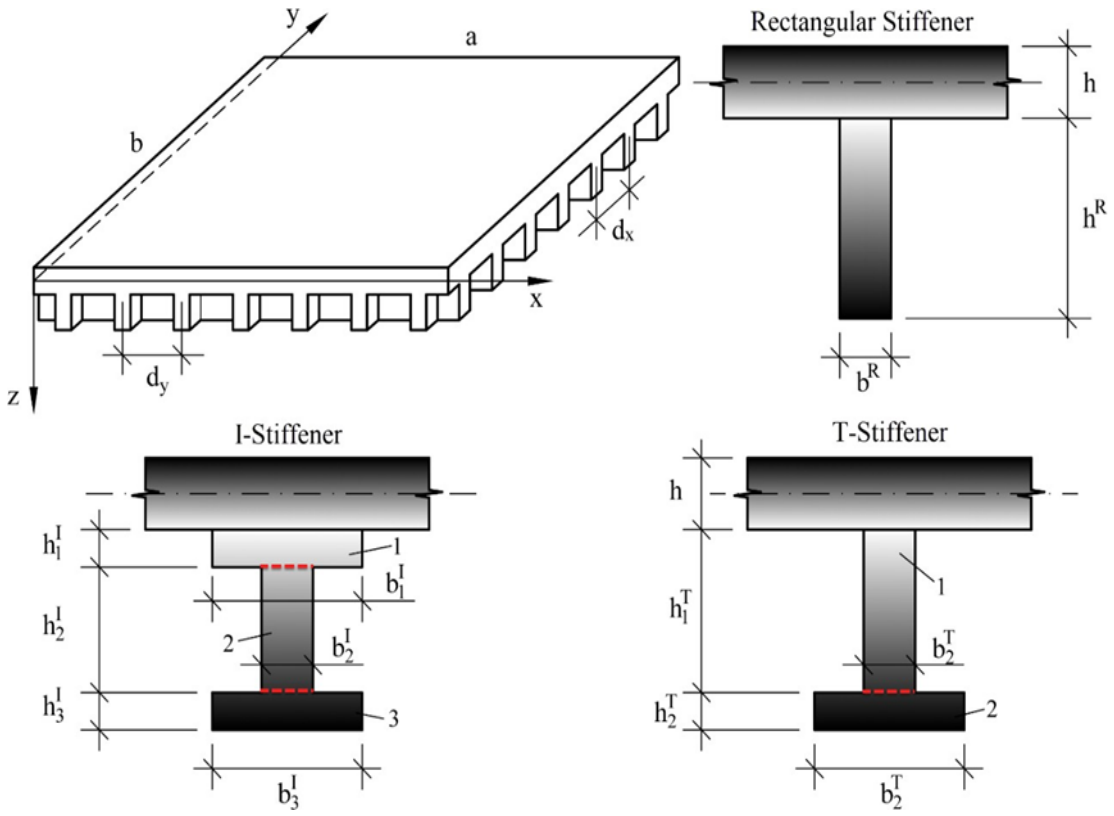

Fig. 1. Geometrical properties and coordinate system of FGM plates stiffened by FGM rectangular, I- and T- stiffeners

The material distribution laws of plate skin and stiffeners are considered in two cases, as

a) Firstly, the upper surface of plate skin and the lower surface of stiffeners are made from the ceramic (Case 1). In this case, the elastic moduli of plate skin and stiffeners are respected to the functions (Fig. 1), as

- For plate skin: $-\frac{h}{2} \le z \le \frac{h}{2}$,

$$E_p = E_c + (E_m - E_c)\left(\frac{2z+h}{2h}\right)^{k_1}. \quad (1)$$

- For stiffeners: $\frac{h}{2} \le z \le \frac{h}{2} + h_g$,

$$E_g = E_m + (E_c - E_m)\left(\frac{2z-h}{2h_g}\right)^{k_2}, \quad (2)$$

where h_g is total height of stiffeners, E_m and E_c are the elastic moduli of metal and ceramic, k_1 and k_2 are the volume fraction index of plate and stiffeners, respectively.

b) Secondly, the upper surface of plate skin and the lower surface of stiffeners are made from

the metal (Case 2). In this case, the elastic moduli of plate skin and stiffeners are respected to the functions, as

- For plate skin: $-\frac{h}{2} \le z \le \frac{h}{2}$,

$$E_p = E_m + (E_c - E_m)\left(\frac{2z+h}{2h}\right)^{k_1}. \quad (3)$$

- For stiffeners: $\frac{h}{2} \le z \le \frac{h}{2} + h_g$,

$$E_g = E_c + (E_m - E_c)\left(\frac{2z-h}{2h_g}\right)^{k_2}. \quad (4)$$

By applying the classical plate theory, the strain components of plate at a distance z from the mid-surface are obtained as

$$\begin{aligned} &\varepsilon_x = \varepsilon_x^0 - z\chi_x, \varepsilon_y = \varepsilon_y^0 - z\chi_y, \\ &\gamma_{xy} = \gamma_{xy}^0 - 2z\chi_{xy}, \end{aligned} \quad (5)$$

where the relations between the strain and displacement at the mid-surface taking into account the von Kármán's geometrical nonlinearity are determined by

$$\begin{aligned} &\varepsilon_x^0 = \frac{\partial u}{\partial x} + \frac{1}{2}\left(\frac{\partial w}{\partial x}\right)^2, \chi_x = \frac{\partial^2 w}{\partial x^2}, \\ &\varepsilon_y^0 = \frac{\partial v}{\partial y} + \frac{1}{2}\left(\frac{\partial w}{\partial y}\right)^2, \chi_\theta = \frac{\partial^2 w}{\partial y^2}, \\ &\gamma_{xy}^0 = \frac{\partial u}{\partial y} + \frac{\partial v}{\partial x} + \frac{\partial w}{\partial x}\frac{\partial w}{\partial y}, \chi_{xy} = \frac{\partial^2 w}{\partial x \partial y}, \end{aligned} \quad (6)$$

where ε_x^0 and ε_y^0 are the normal strains, γ_{xy}^0 is the in-plane shear strain of plate.

By using Eq. (6), the compatibility equation is

$$\frac{\partial^2 \varepsilon_x^0}{\partial y^2} + \frac{\partial^2 \varepsilon_y^0}{\partial x^2} - \frac{\partial^2 \gamma_{xy}^0}{\partial x \partial y} = \left(\frac{\partial^2 w}{\partial x \partial y}\right)^2 - \frac{\partial^2 w}{\partial x^2}\frac{\partial^2 w}{\partial y^2}. \quad (7)$$

Hooke's law for the sandwich FGM plate skin is written as

$$\begin{aligned} &\sigma_x^p = \frac{E_p(z)}{1-\nu^2}(\varepsilon_x + \nu\varepsilon_y), \\ &\sigma_y^p = \frac{E_p(z)}{1-\nu^2}(\varepsilon_y + \nu\varepsilon_x), \\ &\sigma_{xy}^p = \frac{E_p(z)}{2(1+\nu)}\gamma_{xy}. \end{aligned} \quad (8)$$

By using the improved Lekhnitskii's smeared stiffener technique for different stiffener types, the internal force and moment expressions of the FGM plates stiffened by different type of FGM stiffeners are obtained as follows

$$\begin{aligned} &N_x = A_{11}\varepsilon_x^0 + A_{12}\varepsilon_y^0 - B_{11}\chi_x - B_{12}\chi_y, \\ &N_y = A_{12}\varepsilon_x^0 + A_{22}\varepsilon_y^0 - B_{12}\chi_x - B_{22}\chi_y, \\ &N_{xy} = A_{66}\gamma_{xy}^0 - 2B_{66}\chi_{xy}, \end{aligned} \quad (9)$$

$$\begin{aligned} &M_x = B_{11}\varepsilon_x^0 + B_{12}\varepsilon_y^0 - D_{11}\chi_x - D_{12}\chi_y, \\ &M_y = B_{12}\varepsilon_x^0 + B_{22}\varepsilon_y^0 - D_{12}\chi_x - D_{22}\chi_y, \\ &M_{xy} = B_{66}\gamma_{xy}^0 - 2D_{66}\chi_{xy}, \end{aligned} \quad (10)$$

where

$$(A_{ij}, B_{ij}, D_{ij}) = (A_{ij}^p, B_{ij}^p, D_{ij}^p) + (A_{ij}^g, B_{ij}^g, D_{ij}^g), \quad (i, j = 1, 2, 6),$$

are the stiffnesses of plate skin and stiffeners, calculated as

$$\begin{aligned} &A_{ij}^p = \int_{-\frac{h}{2}}^{\frac{h}{2}} Q_{ij}^p dz, \\ &B_{ij}^p = \int_{-\frac{h}{2}}^{\frac{h}{2}} Q_{ij}^p z dz, \quad D_{ij}^p = \int_{-\frac{h}{2}}^{\frac{h}{2}} Q_{ij}^p z^2 dz. \end{aligned} \quad (11)$$

- For rectangular stiffeners

$$\begin{aligned} &A_{kk}^g = \frac{b^R}{d_s}\int_{\frac{h}{2}}^{\frac{h}{2}+h^R} Q_{kk}^g dz, B_{kk}^g = \frac{b^R}{d_s}\int_{\frac{h}{2}}^{\frac{h}{2}+h^R} Q_{kk}^g z dz, \\ &D_{kk}^g = \frac{b^R}{d_s}\int_{\frac{h}{2}}^{\frac{h}{2}+h^R} Q_{kk}^g z^2 dz. \end{aligned} \quad (12)$$

- For T-Stiffeners

$$A_{kk}^g = \frac{b_1^T}{d_s}\int_{\frac{h}{2}}^{\frac{h}{2}+h_1^T} Q_{kk}^g dz + \frac{b_2^T}{d_s}\int_{\frac{h}{2}+h_1^T}^{\frac{h}{2}+h_1^T+h_2^T} Q_{kk}^g dz,$$

$$B_{kk}^{g}=\frac{b_1^{T}}{d_s}\int_{\frac{h}{2}}^{\frac{h}{2}+h_1^{T}}Q_{kk}^{g}zdz+\frac{b_2^{T}}{d_s}\int_{\frac{h}{2}+h_1^{T}}^{\frac{h}{2}+h_1^{T}+h_2^{T}}Q_{kk}^{g}zdz, \quad (13)$$

$$D_{kk}^{g}=\frac{b_1^{T}}{d_s}\int_{\frac{h}{2}}^{\frac{h}{2}+h_1^{T}}Q_{kk}^{g}z^2dz+\frac{b_2^{T}}{d_s}\int_{\frac{h}{2}+h_1^{T}}^{\frac{h}{2}+h_1^{T}+h_2^{T}}Q_{kk}^{g}z^2dz.$$

- For I-Stiffeners

$$A_{kk}^{g}=\frac{b_1^{I}}{d_s}\int_{\frac{h}{2}}^{\frac{h}{2}+h_1^{I}}Q_{kk}^{g}dz + \frac{b_2^{I}}{d_s}\int_{\frac{h}{2}+h_1^{I}}^{\frac{h}{2}+h_1^{I}+h_2^{I}}Q_{kk}^{g}dz+\frac{b_3^{I}}{d_s}\int_{\frac{h}{2}+h_1^{I}+h_2^{I}}^{\frac{h}{2}+h_1^{I}+h_2^{I}+h_3^{I}}Q_{kk}^{g}dz, \quad (14)$$

$$B_{kk}^{g}=\frac{b_1^{I}}{d_s}\int_{\frac{h}{2}}^{\frac{h}{2}+h_1^{I}}Q_{kk}^{g}zdz + \frac{b_2^{I}}{d_s}\int_{\frac{h}{2}+h_1^{I}}^{\frac{h}{2}+h_1^{I}+h_2^{I}}Q_{kk}^{g}zdz+\frac{b_3^{I}}{d_s}\int_{\frac{h}{2}+h_1^{I}+h_2^{I}}^{\frac{h}{2}+h_1^{I}+h_2^{I}+h_3^{I}}Q_{kk}^{g}zdz, \quad (15)$$

$$D_{kk}^{g}=\frac{b_1^{I}}{d_s}\int_{\frac{h}{2}}^{\frac{h}{2}+h_1^{I}}Q_{kk}^{g}z^2dz + \frac{b_2^{I}}{d_s}\int_{\frac{h}{2}+h_1^{I}}^{\frac{h}{2}+h_1^{I}+h_2^{I}}Q_{kk}^{g}z^2dz+\frac{b_3^{I}}{d_s}\int_{\frac{h}{2}+h_1^{I}+h_2^{I}}^{\frac{h}{2}+h_1^{I}+h_2^{I}+h_3^{I}}Q_{kk}^{g}z^2dz, \quad (16)$$

with k is equal to 1 and 2 for $x-$ and $y-$ stiffeners, respectively. d_s is d_x and d_y for $x-$ and $y-$ stiffeners, respectively. The reduced stiffnesses are presented as

$$Q_{11}^{p}=Q_{22}^{p}=\frac{E_p(z)}{1-\nu^2},\quad Q_{12}^{p}=\frac{\nu_p E_p(z)}{1-\nu^2},$$

$$Q_{66}^{p}=\frac{\nu E_p(z)}{2(1+\nu)},$$

$$Q_{11}^{g}=Q_{22}^{g}=\frac{E_g(z)}{1-\nu^2}.$$

The nonlinear equilibrium equation system according to the classical plate theory can be obtained as

$$\frac{\partial N_x}{\partial x}+\frac{\partial N_{xy}}{\partial y}=0,\quad \frac{\partial N_{xy}}{\partial x}+\frac{\partial N_y}{\partial y}=0,$$
$$\frac{\partial^2 M_x}{\partial x^2}+2\frac{\partial^2 M_{xy}}{\partial x\partial y}+\frac{\partial^2 M_y}{\partial y^2} + N_x\frac{\partial^2 w}{\partial x^2}+2N_{xy}\frac{\partial^2 w}{\partial x\partial y}+N_y\frac{\partial^2 w}{\partial y^2}=0. \quad (17)$$

The stress function can be introduced as

$$N_x=\frac{\partial^2\varphi}{\partial y^2},N_y=\frac{\partial^2\varphi}{\partial x^2},N_{xy}=-\frac{\partial^2\varphi}{\partial x\partial y}. \quad (18)$$

The compatibility equation (18) and the 3rd equilibrium equation of (17) can be rewritten respecting two unknown functions: deflection and stress function, presented as

$$A_{11}^{*}\frac{\partial^4\varphi}{\partial x^4}+\left(A_{66}^{*}-2A_{12}^{*}\right)\frac{\partial^4\varphi}{\partial x^2\partial y^2}+A_{22}^{*}\frac{\partial^4\varphi}{\partial y^4} +B_{21}^{*}\frac{\partial^4 w_1}{\partial x^4}+B_{12}^{*}\frac{\partial^4 w}{\partial y^4}-\left(\frac{\partial^2 w}{\partial x\partial y}\right)^2+\frac{\partial^2 w}{\partial x^2}\frac{\partial^2 w}{\partial y^2} +\left(B_{11}^{*}+B_{22}^{*}-2B_{66}^{*}\right)\frac{\partial^4 w}{\partial x^2\partial y^2}=0, \quad (19)$$

$$D_{11}^{*}\frac{\partial^4 w}{\partial x^4}+\left(D_{12}^{*}+D_{21}^{*}+4D_{66}^{*}\right)\frac{\partial^4 w}{\partial x^2\partial y^2} +D_{22}^{*}\frac{\partial^4 w}{\partial y^4}-B_{21}^{*}\frac{\partial^4\varphi}{\partial x^4}-B_{12}^{*}\frac{\partial^4\varphi}{\partial y^4}-\frac{\partial^2\varphi}{\partial y^2}\frac{\partial^2 w}{\partial x^2} -\left(B_{11}^{*}+B_{22}^{*}-2B_{66}^{*}\right)\frac{\partial^4\varphi}{\partial x^2\partial y^2} +2\frac{\partial^2\varphi}{\partial x\partial y}\frac{\partial^2 w}{\partial x\partial y}-\frac{\partial^2\varphi}{\partial x^2}\frac{\partial^2 w}{\partial y^2}=0. \quad (20)$$

The boundary condition of these plates in this paper are considered to be simply supported conditions in all edges. The form of deflection can be modeled by the following function

$$w=W\sin\frac{m\pi x}{a}\sin\frac{n\pi y}{b}, \quad (21)$$

where the buckling modes (m,n) present the half-wave numbers of deflection in longitudinal and transversal directions, respectively.

The stress function form can be obtained by substituting the deflection form into compatibility equation (19), the obtained results are presented as

$$\varphi = \frac{n^2\lambda^2 W^2}{32m^2A_{11}^*}\cos\frac{2m\pi x}{a} + \frac{m^2W^2}{32n^2\lambda^2A_{22}^*}\cos\frac{2n\pi y}{b} - \frac{B}{A}W\sin\frac{m\pi x}{a}\sin\frac{n\pi y}{b} - r_0h\frac{y^2}{2}. \quad (22)$$

Substituting Eqs. (21) and (22) into Eq. (20) and the Galerkin method is applied for the obtained equation, the equilibrium equation can be written in nonlinear algebra equation form, as

$$KW^3 + HW^2 + \left(D + \frac{B^2}{A}\right)W = \frac{a^2h}{\pi^2}r_0m^2W. \quad (23)$$

The postbuckling curve expression of plates can be obtained form Eq. (23), as

$$r_0 = \left[\left(\bar{D} + \frac{\bar{B}^2}{\bar{A}}\right) + \bar{H}\bar{W} + \bar{K}\bar{W}^2\right]\frac{\pi^2h^2}{a^2m^2}, \quad (24)$$

where

$$\bar{A} = Ah,\ B = B/h,\ \bar{D} = D/h^3,$$
$$\bar{H} = H/h^2,\ \bar{K} = K/h,\ \bar{W} = W/h.$$

The critical buckling load of stiffened and unstiffened FGM plates can be obtained by

$$r_0^{upper} = \left(\bar{D} + \frac{\bar{B}^2}{\bar{A}}\right)\frac{\pi^2h^2}{a^2m^2}. \quad (25)$$

The critical buckling load r_0^{cr} can be determined by minimising the r_0^{upper} vs. (m,n).

3. Numerical examples and discussion

The present approach can be validated with the results of Bich et al. [6] and Dung and Nga [7] for stiffened and unstiffened FGM plates. The cross-section of stiffeners are rectangular and the isotropic material are used for stiffeners. As can be observed, the very good agreements can be obtained.

Table 1. Comparisons of present critical buckling loads r_0^{cr} ($\times10^8$N/m^2) with the previous results [6,7] for stiffened and unstiffened FGM plates with isotropic stiffeners $(m,n) = (1,1)$

k	Unstiffened			Stiffened		
	Ref.[6]	Ref.[7]	Present	Ref.[6]	Ref.[7]	Present
0.2	0.320	0.320	0.320	1.350	1.350	1.350
1	0.195	0.195	0.195	1.155	1.155	1.155
5	0.129	0.129	0.129	1.031	1.030	1.031
10	0.117	0.117	0.117	1.024	1.023	1.024

Unless specifically noted, the geometrical and material parameters of FGM plates and stiffeners are chosen as

- Aluminum/Alumina FGM is chosen with the elastic moduli and Poisson ratio of metal and ceramic are $E_m = 70\text{GPa}, E_c = 380\text{GPa}, \nu = 0.3$.

- The geometrical parameters of plate skin are $a = b = 1\text{m}$. Three stiffener types are considered with the same total stiffener height, the same stiffener distance, and the same area of cross-section of stiffeners: $h_g = 0.04\text{m}$, $d_x = d_y = 0.1\text{m}$, and stiffener cross-sectional area $S_S = 0.00006\text{m}^2$. In the case of rectangular stiffeners, the stiffener width is chosen as $b_s^R = 0.0015\text{m}$. The geometrical parameters of I-Stiffeners are $b_1^I = b_3^I = 3\text{mm}$, $h_1^I = h_3^I = 7.5\text{mm}$, $b_2^I = 0.6\text{mm}$, $h_2^I = 2.5\text{cm}$. The T-Stiffener geometrical parameters are $b_1^T = 1\text{mm}$, $h_1^T = 3\text{cm}$, and $b_2^T = 3\text{mm}$, $h_2^T = 1\text{cm}$.

The critical buckling loads $r_0^{cr}\left(\times10^8\text{Pa}\right)$ of FGM plates stiffened by different FGM stiffener types are presented in Table 2. The different a/h ratios and volume fractions of plate skin and stiffeners are also considered.

Table 2. The critical buckling loads $r_0^{cr}\left(\times 10^8 Pa\right)$ of FGM plates stiffened by different metal and FGM stiffener types (Case 1) $(m,n)=(1,1)$

a/h	k_1	Unstiffened	Rectangular Stiffener		I-Stiffener		T-Stiffener	
			$k_2=\infty$	$k_2=k_1$	$k_2=\infty$	$k_2=k_1$	$k_2=\infty$	$k_2=k_1$
50	0.2	1.7326	2.2537	4.2883	2.2908	4.5260	2.4131	5.1508
	1	2.7390	3.2727	4.8663	3.3.97	5.2453	3.4343	5.8011
	5	4.0344	4.5350	5.2319	4.5720	5.7283	4.6915	5.9735
	10	4.5494	5.0373	5.4478	5.0743	5.8457	5.1918	5.9964
80	0.2	0.6768	1.3159	3.7884	1.3751	4.2594	1.5374	4.9573
	1	1.0699	1.7216	3.7164	1.7808	4.1601	1.9461	4.9487
	5	1.5759	2.1999	3.1184	2.2591	3.7924	2.4196	4.1135
	10	1.7771	2.3901	2.9396	2.4493	3.4833	2.6078	3.6845
100	0.2	0.4331	1.1584	3.9407	1.2324	4.4002	1.4210	5.2930
	1	0.6848	1.4234	3.7000	1.4974	4.3513	1.6896	5.1453
	5	1.0086	1.7215	2.7921	1.7956	3.5864	1.9833	3.9583
	10	1.1373	1.8401	2.4844	1.9141	3.1270	2.0997	3.3616

Two cases of metal $(k_2=\infty)$ and FGM stiffeners are investigated. Obliviously, the critical buckling loads of FGM plates stiffened by FGM stiffeners are larger than those of metal stiffeners. Additionally, the critical buckling loads of T-stiffened plates are the largest, and those of rectangular stiffened plates are the smallest. The critical buckling loads of plates increase when the a/h ratio decreases.

Effects of stiffener type and volume fraction index of stiffeners on the critical buckling load of stiffened FGM plates are presented in Fig. 2. As can be seen, compared with the T-stiffened plates and I-stiffened plates, the increased tendencies of the critical buckling load of rectangular stiffened plates are more clear in the small domain of volume fraction.

Effects of number of FGM stiffeners on the postbuckling curved of I-stiffened FGM plates are shown in Fig. 3. The large effects of stiffener number on the postbuckling strength of plates can be observed in this investigation, and the bifurcation type of buckling phenomenon is obtained in all investigated cases.

Fig. 4 presents the postbuckling curves of FGM plates with different stiffener types. Corresponding to the tendencies of critical buckling loads shown in Table 2, the postbuckling strengths of T-stiffened plates are the largest, and those of rectangular stiffened plates are the smallest. Additionally, the tendencies of postbuckling curves of plates with all stiffener type are almost parallel.

In Fig. 5, the stiffener height and width are varied so that the cross-section area of the rectangular stiffener is constant $\left(b^R h^R=\text{const}\right)$. As can be observed, the effects of stiffener height on the critical buckling load and postbuckling strength of plates are greater than those of stiffener width.

Postbuckling curves of stiffened and unstiffened FGM plates with different distribution laws (Case 1 and 2) are shown in Fig. 6. With the linear distribution laws $(k_1=k_2=1)$, the postbuckling curves of unstiffened plates in two cases coincide together. Oppositely, the postbuckling curves of stiffened plates in Case 1

are much upper than that in Case 2. It can be explained that ceramic is distributed far from the neutral surface of structure in case 1 and near the neutral surface in case 2. It leads to a large difference in stiffnesses in the two cases.

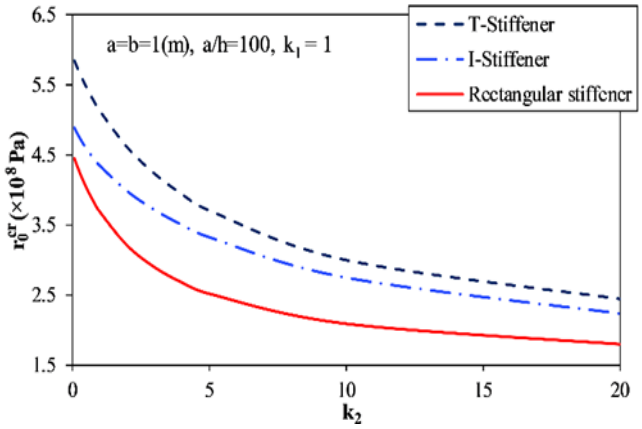

Fig. 2. Effects of stiffener type and volume fraction index of stiffeners k_2 on the critical buckling load of stiffened FGM plates (Case 1)

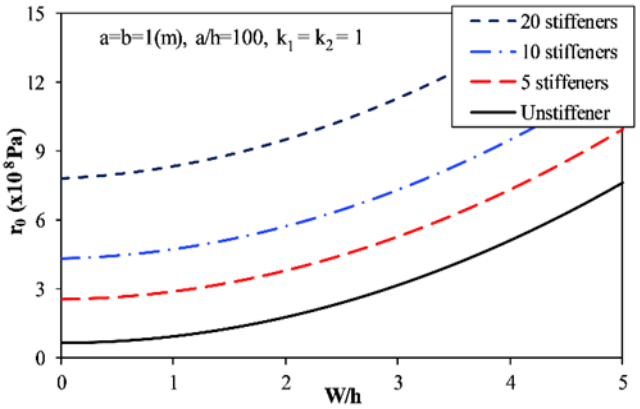

Fig. 3. Effects of number of stiffeners on the postbuckling curves of I-stiffened FGM plates (Case 1)

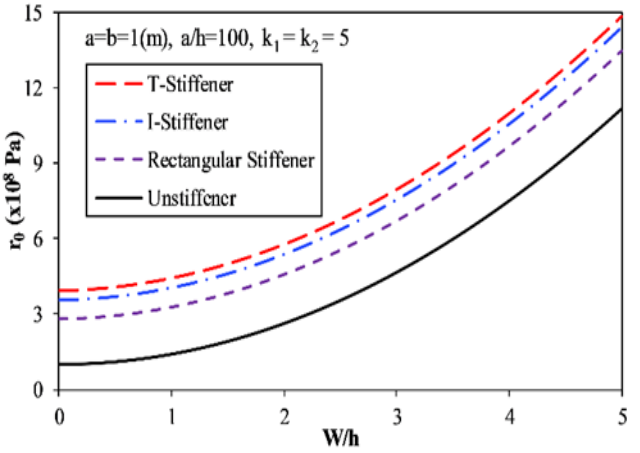

Fig. 4. Effects of number of stiffener type on the postbuckling curves of FGM plates (Case 1)

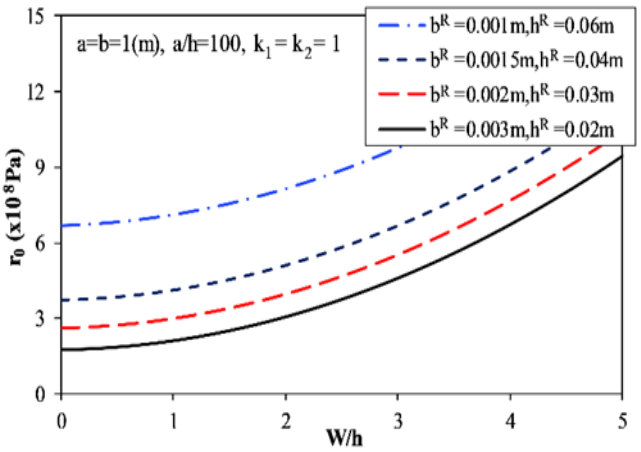

Fig. 5. Effects of geometrical parameters of rectangular stiffeners on the postbuckling curves of FGM plates (Case 1)

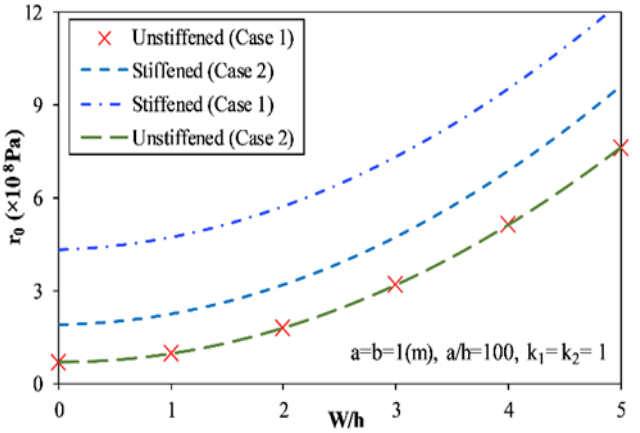

Fig. 6. Postbuckling curves of stiffened and unstiffened FGM plates with different distribution laws (Case 1 and 2)

4. Conclusion

Based on the classical plate theory with von Karman nonlinearities, the improved smeared stiffeners technique for different stiffener types (rectangular, T- and I-Stiffener types) are presented, and Galerkin method is applied, the closed-form of the critical buckling load and postbuckling curves of stiffened FGM plates under compression loads are presented in this paper. The numerical results present the strong effects of stiffener types, material distribution laws, geometrical and material properties of plates on the critical buckling load of plates.

References

[1] Koizumi M. The concept of FGM. Ceramic Trans, Funct Grad Mater 1993; 34: 3–10

[2] Reddy JN. Analysis of functionally graded platesInt J Numer Methods Eng 2000; 47: 663–684

[3] Yang J and Shen HS. Nonlinear bending analysis of shear deformable functionally graded plates subjected to thermo-mechanical loads under various boundary conditions. Compos Part B-Eng 2003; 34: 103-115

[4] Taczała M, Buczkowski R and Kleiberc M. Nonlinear buckling and post-buckling response of stiffened FGM plates in thermal environments. Compos Part B-Eng 2017; 109: 238-247

[5] Shen HS. Thermal postbuckling behavior of shear deformable FGM plates with temperature-dependent properties. Int J Mech Sci 2007; 49: 466-478

[6] Bich DH, Dung, DV, Nam, VH. Nonlinear dynamical analysis of eccentrically stiffened functionally graded cylindrical panels. Compos Struct 2012; 94: 2465–2473

[7] Dung DV, Nga NT. Buckling and postbuckling nonlinear analysis of imperfect FGM plates reinforcedby FGM stiffeners with temperature-dependent properties based on TSDT, Acta Mech 2016); 227(8): 2377–2401

[8] Nam VH, Dong DT, Phuong NT, Tuan HD. Nonlinear thermo-mechanical stability of multilayer-FG plates reinforced by orthogonal and oblique stiffeners according to FSDT. J Reinf Plast Compos 2019; 38(11): 521-536

[9] Dong DT, Nam VH, Trung NT, Phuong NT, Hung VT. Nonlinear thermomechanical buckling of sandwich FGM oblique stiffened plates with nonlinear effect of elastic foundation. J Thermoplast Compos Mater 2020. doi:10.1177/0892705720935957